

Time delay of resistive-state formation in superconducting stripes excited by single optical photons

J. Zhang,* W. Słysz,† A. Pearlman, A. Verevkin, and Roman Sobolewski‡

Department of Electrical and Computer Engineering and Laboratory of Laser Energetics, University of Rochester, Rochester, New York 14627-0231

O. Okunev, G. Chulkova, and G. N. Gol'tsman

Department of Physics, Moscow State Pedagogical University, Moscow 119435, Russia

(Received 5 August 2002; published 28 April 2003)

We have observed a $65(\pm 5)$ -ps time delay in the onset of a resistive-state formation in 10-nm-thick, 130-nm-wide NbN superconducting stripes exposed to single photons. The delay in the photoresponse decreased to zero when the stripe was irradiated by multi-photon (classical) optical pulses. Our NbN structures were kept at 4.2 K, well below the material's critical temperature, and were illuminated by 100-fs-wide optical pulses. The time-delay phenomenon has been explained within the framework of a model based on photon-induced generation of a hotspot in the superconducting stripe and subsequent, supercurrent-assisted, resistive-state formation across the entire stripe cross section. The measured time delays in both the single-photon and two-photon detection regimes agree well with theoretical predictions of the resistive-state dynamics in one-dimensional superconducting stripes.

DOI: 10.1103/PhysRevB.67.132508

PACS number(s): 74.78.-w

Recently proposed superconducting single-photon detectors (SSPDs), based on ultrathin, submicrometer-width NbN superconducting stripes, are characterized by picosecond response times, high quantum efficiency, broadband single-photon sensitivity, and extremely low dark counts.¹⁻³ The devices immediately found a variety of applications ranging from noninvasive testing of very-large-scale integrated circuits⁴ to quantum cryptography.⁵ Their single-photon-counting ability has been interpreted within a phenomenological hot-electron photoresponse model proposed in Ref. 1, and elaborated upon in Ref. 6. The model describes the formation of a hotspot,⁷ right after the single-photon absorption event, followed by the in-plane growth of a resistive hotspot area due to the highly efficient multiplication process of excited quasiparticles in the NbN film.⁸ During this stage, however, the resistive state does not appear across the superconducting stripe because the size of a single hotspot, created by an optical photon, is significantly smaller than our stripe width.² The resistive state appears due to a supplementary action of the device bias current density j , which needs to be close to the stripe critical current density j_c . After the supercurrent is expelled from the resistive hotspot region, the bias current density in the stripe “sidewalks” j_{sw} exceeds j_c , resulting in a penetration of the electric field in the sidewalk areas of the stripe.⁶ As a result, we observe a voltage pulse, which reflects the initial act of photon capture.

The mechanism of the hotspot formation in superconducting films was earlier implemented in high-energy particle detectors.⁹ However, these detectors had large areas and were sensitive only to highly energetic excitations. The resulting response was slow (at least hundreds of ns), since the particle absorption led to the strong perturbation of the stripe's vortex structure and the significant phonon-system heating. In our nanometer-width detectors, vortices cannot appear; at the same time, our films are thinner than the phonon mean free path, so the phonon escape time is minimized.

The resistive-state formation process presented above should lead to an observable time delay t_d in the superconducting stripe resistive photoresponse.¹⁰ This delay, in turn, if measured, would give us a direct confirmation of a supercurrent-enhanced, hotspot-induced photoresponse mechanism of our SSPD.¹ The latter is the main experimental goal of this work.

The dynamics of the resistive-state formation in a photon-illuminated, ultrathin (two-dimensional) superconducting stripe depends on the radiation flux density incident on the device and the bias current density, as schematically illustrated in Fig. 1. At relatively high (macroscopic) incident photon fluxes, a large number of hotspots are simultaneously formed in our stripe [Fig. 1(a)]. In this case, the hotspots overlap with each other across the stripe cross section. Since the stripe thickness d is comparable with the coherence length ξ , we can assume that for overlapping hotspots, a resistive barrier is instantaneously formed across the NbN stripe and, as a result, a voltage signal is generated within the electron thermalization time of 6.5 ps.¹¹ When the photon flux is decreased, the hotspots become isolated [Fig. 1(b)]. Finally, for an incident flux containing one or less than one absorbed photon per pulse, we can expect that, at best, only one resistive hotspot will be formed in our stripe [Fig. 1(c)]. As we mentioned above, in the single-photon regime we postulate that the formation of a macroscopic resistive barrier can be realized only when j_{sw} surpasses j_c , which is associated with a macroscopic current redistribution and should lead to a measurable t_d in the resistive state formation, corresponding to the time period between the initial hotspot appearance and the eventual development of a resistive barrier across the entire cross section of the superconducting stripe.

Even if the two-photon detection mechanism^{1,2} does not correspond exactly to the situation presented in Fig. 1(b), since the hotspots may partially overlap, or coincide, we should still observe—as in the single-photon regime—a non-

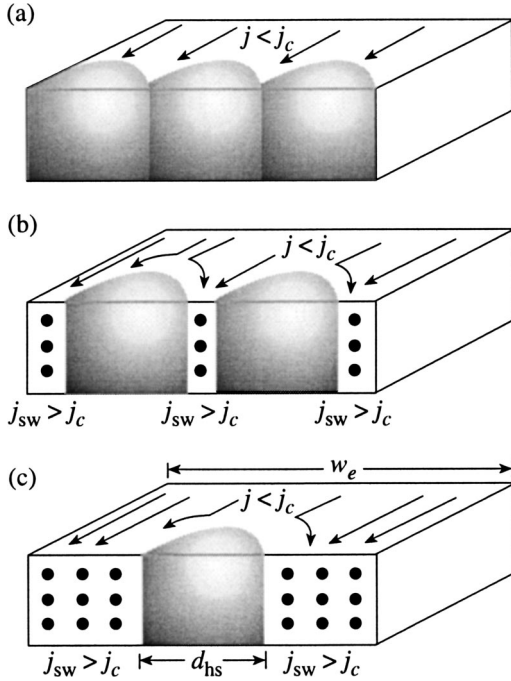


FIG. 1. Schematic presentation of the dynamics of resistive-barrier formation across a superconducting stripe: (a) high (macroscopic) incident photon flux, (b) the two-photon regime, leading to the generation of two hotspots in the superconducting stripe cross section, and (c) the single-photon regime.

zero t_d for the voltage pulse generation. In terms of the superconductor dynamics, t_d is the time required for a superconductor energy gap Δ to be reduced to zero by the current in the sidewalks and, for $j_{sw} > j_c$ can be calculated using the Tinkham model¹² as

$$t_d = 2\tau_\Delta \int_0^1 \frac{f^4}{[2j_{sw}/(3\sqrt{3}j_c)]^2 + f^6 - f^4} df, \quad (1)$$

where $\tau_\Delta \approx 2.41\tau_E/\sqrt{1-T/T_c}$ is the gap relaxation time¹⁰ (τ_E is the inelastic electron-phonon collision time at the Fermi level at T_c) and $f = \Delta/\Delta_0$ [$\Delta_0 = \Delta(T=0)$].¹²

The devices used in our experiments were $4 \times 4\text{-}\mu\text{m}^2$ -area, meander-type, NbN stripes with $d = 10$ nm, a nominal width $w = 130$ nm, and a total length of about $30 \mu\text{m}$. The structures were superconducting at $T_c = 10.5$ K and exhibited $j_c = 6 \times 10^6$ A/cm² at 4.2 K. Details of their fabrication and implementation as SSPDs are described in Refs. 2 and 13; here we only wanted to stress that with the constant j_c , I_c of the meander is determined by its narrowest segment, and, according to our supercurrent-enhanced, resistive-state formation model, the narrowest segments of the stripe contribute the most to the SSPD photoresponse.² The atomic force microscope images showed that irregularities in our stripes were up to 25 nm, close to the cantilever resolution limit.¹³ The I_c of the meander structures, measured at 4.2 K, was typically 60% lower than I_c for the control (short) stripe fabricated in the same process. Thus, to account for the width variations and the fact that different parts of the detector stripe (e.g., meander

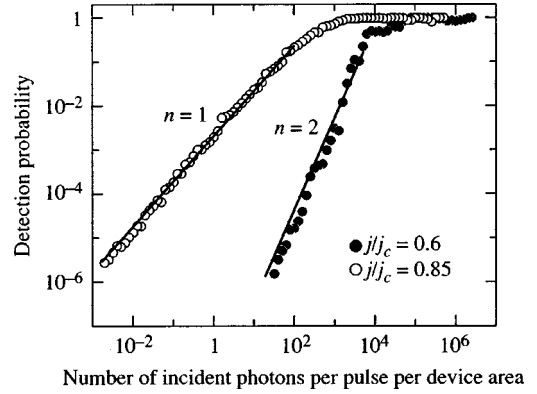


FIG. 2. Detection probability of 82-MHz repetition rate laser pulses vs number of incident photons per laser pulse, measured at two normalized current biases: $j/j_c = 0.85$ (open circles) and $j/j_c = 0.6$ (closed circles). Solid lines are guides to the eye and correspond to the single-photon detection regime (linear dependence on flux; $n=1$) and the two-photon detection regime (quadratic dependence on flux; $n=2$).

turns) contribute differently to the total photoresponse, we introduce the effective stripe width w_e , corresponding to the detector segments most active in the resistive-state formation and photon detection, and we estimate w_e to be 80 nm.

Our devices were mounted inside a cryostat on a 4.2-K cold base plate, wire bonded to a 50- Ω microwave stripe line, and connected to the bias and output circuitry through a cryogenic bias tee.^{3,5} As optical excitation, we used 100-fs-wide pulses from a Ti:sapphire laser with a wavelength of 810 nm and a repetition rate of 82 MHz. The laser radiation power was attenuated down to a picowatt range using banks of neutral density filters. Voltage pulses generated by our SSPDs were amplified by a room-temperature amplifier and fed either to a synchronously triggered Tektronix 7404 single-shot digital oscilloscope, or to a fast photon counter. The ~ 100 -ps, real-time resolution of our system was limited by the 0–4-GHz bandwidth of the oscilloscope (the amplifier had a bandwidth of 0.01–12 GHz). On the other hand, the relative-time resolution, e.g., the delay between the photoresponse pulses generated under different photon excitations, was below ~ 10 ps, due to the low jitter of our laser and the digital accumulation procedure of acquired pulses (with no averaging) implemented in our oscilloscope.

A fast photon counter was used in our experimental setup to perform the statistical data analysis and to determine the single-photon, two-photon, or multiphoton regimes of operation of our devices, as described in detail in Refs. 1 and 2. Figure 2 presents the two dependences of the SSPD counting probability vs the averaged number of photons incident on the device area for two different biasing conditions. The actual values for the x axis were obtained knowing the amount of attenuation in our optical path, the beam size (typically $\sim 100 \mu\text{m}^2$), the incident energy per pulse of 810-nm photons, and, of course, the actual attenuation level of neutral density filters. As we discussed before,^{1–3} the Poisson probability $P(n)$ of absorbing n photons from a given pulse with a mean number of m photons, for $m \ll 1$ simplifies to $P(n) \sim m^n/n!$. Consequently, the data in Fig. 2 show that, for low

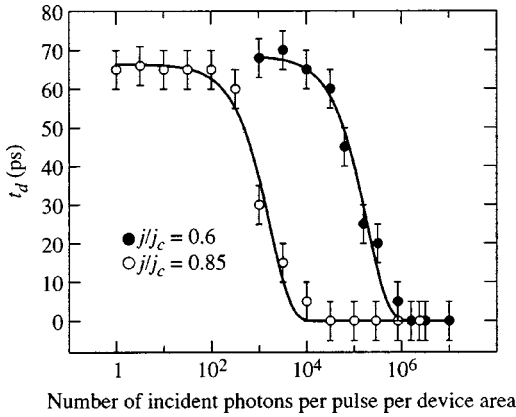


FIG. 3. Experimental time delay t_d of the resistive-state formation in a NbN superconducting stripe as a function of the number of incident photons per laser pulse per device area. Open circles correspond to t_d measured when the stripe was biased with $j/j_c = 0.85$ (single-photon regime), while closed circles represent $j/j_c = 0.6$ and the two-photon regime. Solid lines are guides to the eye. The measurement error is ± 5 ps.

photon fluxes, we have a true single-photon detection ($n = 1$) at the normalized bias $j/j_c = 0.85$, as the detection probability is proportional to m , while at $j/j_c = 0.6$ the detector operates in the quadratic, two-photon detection regime ($n = 2$). It can be noticed that the two-photon dependence is shifted into much higher photon fluxes, since the probability of two-photon detection is significantly lower than that for single photons. The experimental quantum efficiency (QE), defined as the counting probability at the 1 photon/pulse level, is about 0.1% for $j/j_c = 0.85$ and the counting rate saturation level of 82 MHz (repetition rate of laser pulses) is reached at about 10^4 incident photons/pulse, both values are typical for our $4 \times 4\text{-}\mu\text{m}^2$ SSPDs.^{2,3}

Figure 3 presents the main result of our research, the experimental time delay t_d of the photoresponse signal generation versus the number of photons per pulse, incident on the device. The data are presented for the two bias conditions: $j/j_c = 0.85$ (open circles) and $j/j_c = 0.6$ (closed circles), which, as we have already shown in Fig. 2, correspond to the SSPD single-photon and two-photon regimes of operations, respectively. We observe that for large incident photon fluxes ($> 10^6$ is the macroscopic number of photons per pulse), t_d does not depend on the radiation flux. Clearly, this situation corresponds to the multihotspot generation case presented in Fig. 1(a). We use this condition as a reference and refer to as $t_d = 0$. When the incident flux is decreased, the arrivals of the photoresponse signals start to be time delayed with respect to the multiphoton response. Finally, for the lowest flux densities, t_d saturates. For the $j/j_c = 0.85$ bias, t_d increases rapidly in the 10^3 – 10^2 incident photon flux range, which, for a QE of 0.1%, corresponds to ~ 1 photon/pulse absorbed by the SSPD. Thereafter, the arrival of the photoresponse pulse is not further delayed in time scale, even if we attenuated the flux down to 10^{-3} absorbed photons/pulse. We interpret the measured time interval between the multi-photon and the single-photon responses, $\Delta t_d = 65 \pm 5$ ps, as the time needed for supercurrent redistribution around a single, photon-

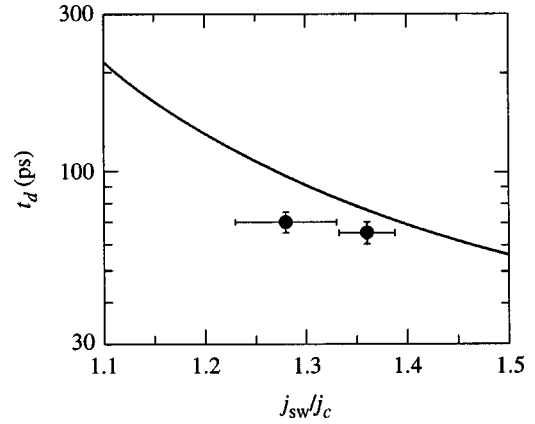


FIG. 4. Time delay t_d as a function of the normalized current j_{sw}/j_c in the sidewalks of the superconducting stripe. The two measured values of Δt_d (solid circles) correspond to the single-hotspot and two-hotspot formation at $j_{sw}/j_c = 1.36$ and $j_{sw}/j_c = 1.28$, respectively. The solid line represents the Tinkham theoretical prediction, calculated using Eq. (1). The horizontal error bars are calculated for the hotspot-diameter variations of 30 ± 1 nm.

created hotspot and subsequent formation of the resistive barrier for $j_{sw} > j_c$ [see Fig. 1(c)].

For the $j/j_c = 0.6$ bias, according to Fig. 2, the probability of detecting a single, 810-nm photon by our $4 \times 4\text{-}\mu\text{m}^2$ device is negligibly small; thus, we need at least two photons in order to generate the resistive response. As we see in Fig. 3, the observed behavior (closed circles) is very similar to that measured for $j/j_c = 0.85$, we can clearly identify the time-delay effect and find $\Delta t_d = 70 \pm 5$ ps. The main difference is that the observed photoresponse delay is shifted into significantly higher levels of the incident photon flux. The value of t_d starts to be nonzero for $\sim 10^6$ incident photons/pulse, and it flattens below 10^4 photons/pulse. The latter value is very consistent with the two-photon ($n = 2$) detection probability dependence observed in Fig. 2.

The data presented in Figs. 2 and 3 show that, in full accordance with the proposed earlier current-enhanced, hotspot-induced photoresponse model,¹⁻³ the voltage signal generated across our superconducting stripe becomes time delayed as we lower the incident photon flux and the device is transferred from the classical, intensity detection mode to the quantum one- or two-photon regime.

Finally, we compare our experimental results with t_d calculated for our experimental conditions, using Eq. (1) and $\tau_E \approx 10$ ps.¹¹ The current density in the sidewalks in the narrowest (most active) segments of the meander can be calculated as: $j_{sw} = j[w_e/(w_e - d_{hs})]$, where $d_{hs} \approx 30$ nm is the diameter of the hotspot generated by a single 810-nm photon.² Thus, for the experimental $j/j_c = 0.6$ condition, $j_{sw}/j_c = 0.96$, and is subcritical in the single-hotspot regime. However, doubling the hotspot size¹⁴ gives $j_{sw}/j_c = 1.28$, which is sufficient to generate a resistive barrier across our stripe. In a similar manner, when $j/j_c = 0.85$, j_{sw}/j_c is supercritical and reaches 1.36, when the single hotspot is formed. Figure 4 shows the t_d dependence on j_{sw}/j_c . The solid line represents the Tinkham model,¹² while the two closed circles refer to our measured Δt_d values, corresponding to the single-

hotspot ($j_{sw}/j_c=1.36$) and double-hotspot ($j_{sw}/j_c=1.28$) conditions, respectively. We note that our experimental values are reasonably close to the theoretical prediction, remembering that the Tinkham theory is applicable for one-dimensional clean superconductors, while our 10-nm-thick NbN films are in the dirty limit and the “sidewalks” are only quasi-one-dimensional. In addition, the discrepancy can be related to the accuracy of our w_e estimation. Within the framework of the Tinkham model, t_d should not depend directly on the number of incident photons, in agreement with the experiment.

In conclusion, we observed the time-delay effect in the resistive-state response in ultrathin, submicrometer-width superconducting stripes, excited by single optical photons. The

observed phenomenon directly shows that the resistive state across two-dimensional superconducting stripes upon absorption of an optical photon is due to photon-induced hotspot formation and to the subsequent redistribution of the supercurrent into the sidewalks of the stripe. Our measurements agree well with a theoretical prediction based on the Tinkham model of the resistive-state formation in superconducting stripes under the supercurrent perturbation.¹²

The authors thank Ken Wilsher for many very valuable discussions. This work was funded by the NPTest, San Jose, CA. Additional support was provided by the US Air Force Office for Scientific Research Grant No. F49620-01-1-0463 (Rochester) and by the RFBR Grant No. 02-02-16774 (Moscow).

*Corresponding author.

Email address: jinzhan@ece.rochester.edu; also at the Materials Science Program, University of Rochester, Rochester, New York 14627.

†Also at the Institute of Electron Technology, PL-02668 Warszawa, Poland.

‡Also at the Institute of Physics, Polish Academy of Sciences, PL-02668 Warszawa, Poland.

¹G. N. Gol'tsman *et al.*, Appl. Phys. Lett. **79**, 705 (2001).

²A. Verevkin *et al.*, Appl. Phys. Lett. **80**, 4687 (2002).

³R. Sobolewski, A. Verevkin, A. Lipatov, G. N. Gol'tsman, and K. Wilsher, IEEE Trans. Appl. Supercond. (to be published).

⁴S. Somani *et al.*, J. Vac. Sci. Technol. B, Microelectron. Nanometer Struct. **19**, 2766 (2001).

⁵A. Verevkin *et al.*, in *Free-Space Laser Communication and Laser Imaging II*, edited by J. C. Ricklin and D. G. Voelz (SPIE, Bellingham, WA, 2002), Proc. SPIE **4821**, 447 (2002).

⁶A. D. Semenov, G. N. Gol'tsman, and A. A. Korneev, Physica C **351**, 349 (2001).

⁷A. M. Kadin and M. W. Johnson, Appl. Phys. Lett. **69**, 3938 (1996).

⁸K. S. Il'in *et al.*, Appl. Phys. Lett. **73**, 3938 (1998).

⁹R. Wedenig *et al.*, Nucl. Instrum. Methods Phys. Res. A **433**, 646 (1999); A. Gabutti, K. E. Gray, and R. G. Wagner, Nucl. Instrum. Methods Phys. Res. A **289**, 274 (1990).

¹⁰D. J. Frank *et al.*, Phys. Rev. Lett. **50**, 1611 (1983); D. J. Frank and M. Tinkham, Phys. Rev. B **28**, 5345 (1983).

¹¹K. S. Il'in *et al.*, Appl. Phys. Lett. **76**, 2752 (2000).

¹²M. Tinkham, *Introduction to Superconductivity*, 2nd ed., International Series in Pure and Applied Physics (McGraw-Hill, New York, 1996).

¹³G. N. Gol'tsman *et al.*, IEEE Trans. Appl. Supercond. (to be published).

¹⁴In the case when two hotspots are present in the film, we have taken the average effective size of the double hotspot across the cross section of the NbN stripe to be $\sqrt{2d_{hs}^2}$, in order to take into account a possible overlap between the hotspots.